Tellus (2000), 52B, 828–842
Printed in UK. All rights reserved

TELLUS
ISSN 0280–6509

Cloud condensation nuclei and cloud droplet measurements during ACE-2

By JEFFERSON R. SNIDER[1]* and JEAN-LOUIS BRENGUIER[2], [1]*University of Wyoming, Department of Atmospheric Science, Laramie, Wyoming, USA;* [2]*Meteo-France, CNRM/GMEI, Toulouse, France*

(Manuscript received 11 February 1999; in final form 27 September 1999)

ABSTRACT

During the 2nd Aerosol Characterization Experiment (ACE-2), relationships between stratocumulus cloud properties and aerosols were examined. Here, the relevant measurements including the cloud condensation nuclei (CCN) activation spectrum, updraft velocity, cloud microphysical and aerosol properties are presented. It is shown that calculations of droplet concentration based on updraft velocity and the CCN activation spectrum are consistent with direct observations. Also discussed is an apparent disparity among measurements of the CCN activation spectrum, the accumulation mode size distribution, and the composition of the submicrometric aerosol. The observed consistency between CCN, updraft and cloud droplets is a necessary refinement; however, extended analyses of the ACE-2 data set are needed to guide improvements in model simulations of the interaction between aerosols and cloud microphysics. In particular, there is need for an examination of aerosol size spectra and chemical composition measurements with a view towards validating droplet activation schemes which relate the aerosol and cloud dynamical properties to cloud albedo.

1. Introduction

Cloud droplet concentration (N_d) and cloud depth control the albedo of stratocumulus cloud layers (Twomey, 1977; Boers and Mitchell, 1994; Brenguier et al., 1999). These cloud systems strongly influence solar energy input into the earth/atmosphere system. Factors which control N_d in stratocumulus include the physical and chemical properties of the aerosol (Pruppacher and Klett, 1997), updraft velocity at cloud base (Twomey and Warner, 1967; Gultepe et al, 1996; Yum et al., 1998), entrainment (Brenguier et al., 1999) and drizzle formation (Albrecht, 1989). Since a substantial fraction of the aerosol in the marine stratocumulus environment originates from anthropogenic activity, there is a pressing need to develop validated schemes which quantify the stratocumulus/aerosol interaction. These schemes can then be applied to diagnose both weather and climate in numerical simulation models. Improving the accuracy of these models is a principal goal of the 2nd Aerosol Characterization Experiment (ACE-2) (Raes et al., 2000).

The development of realistic parameterizations of stratocumulus albedo is confounded by several factors. Foremost of these is the problem of describing cloud formation within a numerical simulation. Of importance here are the issues of condensate distribution in both the vertical and horizontal dimensions as well as the updraft velocity. Also of importance is the problem of predicting the concentration of aerosol particles capable of nucleating condensation over a range

* Corresponding author: Department of Atmospheric Science, University of Wyoming, Laramie, WY, 82071-3038, USA.
e-mail: jsnider@uwyo.edu

of vapor supersaturations (Bigg, 1986; Quinn et al., 1993; Covert et al., 1998). The latter relationship is commonly referred to as the cloud condensation nucleus activation spectrum. A related issue is the problem of going from predictions of the aerosol size spectrum, diagnosed using detailed models of aerosol source and sink processes (Raes, 1995; Fitzgerald et al., 1998), to the CCN activation spectrum and therefore droplet concentration for a prescribed value of the updraft velocity (Twomey, 1959; Feingold and Heymsfeld, 1992; Ghan et al., 1993; Cohard et al., 1998).

Here we present airborne measurements, obtained from the Meteo-France Merlin aircraft during the ACE-2 field campaign, which are relevant to the previously discussed research challenges. This research was conducted during June and July 1997. Measurements were made near the Canary Islands, Spain, in a region characterized by persistent stratocumulus clouds. The microphysical and optical properties of these clouds are frequently perturbed by aerosols advected from continental sources (Brenguier et al., 1999). Our specific objectives are to describe measurements of the CCN activation spectrum made with a new airborne counter, to present a comparison of these measurements to both condensation nuclei (CN) and accumulation mode aerosol measurements, to examine relationships between measurements of vertical velocity and cloud microphysical properties, and to investigate consistency between derived values of N_d and observations obtained from a cloud in situ measurement system. The derived values of N_d were inferred by differencing below-cloud and cloud-interstitial CCN concentrations and were also calculated using an analytical relationship developed by Twomey (1959). We show a consistent relationship between the prediction of the Twomey equation and the in situ observations of cloud droplet concentration.

2. Measurements

The Merlin is a twin turbo-prop aircraft equipped for tropospheric measurements, especially in clouds. In this paper we analyze cloud microphysical properties measured by the fast-FSSP (Brenguier et al., 1998). For ACE-2 this instrument was located external to the aircraft fuselage, to the left and below the pilot. Aerosol measurements were obtained using the University of Wyoming static diffusion counter (WYOCCN), two CN counters (model 3760A, TSI, Inc., St. Paul, MN), and a PCASP-100X (PMS Inc., Boulder, CO). Of the two CN counters, we utilize data from the model 3760A which has a detection limit of 0.01 μm (Franz Schröder, personal communication, 1999). Based on calculations presented in Section 4, a 0.01 μm ammonium sulfate particle will activate to form cloud droplets at a water vapor supersaturation equal to 6%. We plot our CN measurements at 6% when comparing the CCN and CN results. The PCASP data was analyzed using bin sizing information obtained from the manufacturer.

Aerosol sampled by both the CN counters and the PCASP entered the Merlin via a reverse-flow inlet. This inlet is similar to the design developed by Schröder and Ström (1997). For the current application (airspeed 90 m/s and flight altitudes less than 1.5 km) the maximum transmitted particle diameter is expected to be about a factor of 2 larger than the cut size inferred by Schröder and Ström (0.5 to 1.0 μm). The WYOCCN sampled via a forward facing inlet which was mounted within a velocity diffuser. The diffuser has a front opening of 12 mm and an opening angle of 14°. This reduces the air speed by a factor of 12 so that sampling was conducted quasi-isokinetically. Here the maximum transmitted particle size is expected to be larger than that for the reverse-flow inlet. Calculations based on impaction theory show that the size cut is 8 μm (Foltescu et al., 1995), but the actual size cut is expected to be smaller than this estimate (Huebert et al., 1990). Our conclusions are not sensitive to the exact values of either of the size-cut diameters. Both inlets were located along the top centerline of the Merlin, 1 m forward of the tail. All of the aerosol measurements were made inside the Merlin at a temperature at least 15°C warmer than the ambient values. Hence, we have assumed that most of the chemically-bound water was evaporated prior to detection by the CN and PCASP.

The WYOCCN is similar to other static diffusion thermal-gradient diffusion instruments (Lala and Juisto, 1977). A 670 nm solid-state laser illuminates droplets as they grow inside a disk-shaped chamber and a photodetector measures the amount of scattered light. The photodetector voltage is the primary measurement of the

WYOCCN and is recorded continuously at 1 Hz. A vapor gradient is produced in the chamber by cooling the bottom plate thermoelectrically. Both the top and the bottom plate are kept wet for up to 2 h using saturated blotter paper. To obtain a CCN measurement at a single supersaturation requires less than 40 s. The measurement cycle consists of a 5 to 10 s adjustment of the temperature difference between the top and bottom plates, a 5 s flush of the chamber with a new air sample (flow rate 3 L/min), and a 20 s interval that is used to monitor the development of the cloud within the chamber.

Calibration of the WYOCCN consists of establishing the relationship between the number of water droplets, evaluated using a video camera, and the photodetector voltage. Since the volume of the laser beam which is viewed by the video camera is small (0.071 cm^{-3}), numerous measurements of the droplet number and photodetector voltage are needed to establish a robust relationship between these 2 quantities. This calibration does change with applied supersaturation (S) and this dependence is parameterized using data collected at 0.2, 0.4, 0.8, and 1.6% supersaturation.

Uncertainties in the CCN concentration measurement were evaluated 3 months after the ACE-2 field campaign (Snider et al., 2000). This work was conducted using quasi-monodisperse ammonium sulfate aerosols. The test aerosol was characterized using both the WYOCCN and a scanning mobility particle-sizing system (SMPS, TSI, Inc., St. Paul, MN). The selected aerosol sizes ranged between 0.04 and 0.07 μm and the WYOCCN was programmed to make measurements at supersaturations between 0.2 and 1.6%, thus covering the complete range of particle activation. The average relative bias corresponding to the cumulative number concentration measured by the WYOCCN and that derived from the SMPS was 7%. Variation about the average bias was characterized by a standard deviation equal to $\pm 56\%$. In Snider et al. (2000) we attribute this variability to comparable uncertainties in the WYOCCN CCN measurement and in the SMPS measurement of the reference ammonium sulfate size distribution. Our best estimate of the CCN measurement error, including both random and systematic uncertainties, is $\pm 40\%$. Poisson counting error associated with the WYOCCN measurement becomes a significant source of uncertainty at low concentrations ($\pm 30\%$ at 30 cm^{-3}), but was not of significance in the laboratory tests analyzed by Snider et al. (2000).

Local values of the vertical wind velocity (w) were obtained from measurements of the airflow made by differential-pressure sensors mounted on the nose radome of the Merlin (Brown et al., 1983). These were converted to the earth-relative frame using aircraft motion data obtained from an inertial navigation system. The derived values of w are affected by imprecision in the platform-relative and earth-relative velocity measurements. Also of concern are the results of Paluch and Lenchow (1991) which show the potential for systematic error in w when using data derived from flight segments conducted during rapid ascent/descent maneuvers, during turns, and in regions of patchy cloud. These sources of uncertainty were minimized by considering only level-flight cloud traverses for the acquisition of w. With the exception of observations obtained from a cumulus cloud studied on 4 July, the vertical velocity measurements used in the droplet activation calculation were adjusted by removing the median value of w. The mesoscale component of the vertical wind, and biases resulting from the time-integration of the aircraft acceleration, are removed by this procedure. For the selected data segments, the uncertainty in the 2nd moment of the w probability density function is thought to be on the order of ± 0.1 m/s. This estimate is based on field intercomparison tests that involved the NCAR Electra and 3 other meteorological research aircraft (Dobosy et al., 1997). The air motion measurement system employed on the Merlin is based on the NCAR Electra design (Brown et al., 1983).

3. Overview

In this paper we consider data collected by the Merlin during June and July of 1997. Nine research flights are analyzed. These were selected from the Merlin archive based on 2 criteria: (1) the existence of stratocumulus or cumulus cloud sections of minimum duration 1 min, and (2) the acquisition of below-cloud CCN measurements. The selected flights are summarized in Table 1. The data set consists of 6 missions conducted around a 60 km square located at least 50 km

Table 1. *Below-cloud aerosol measurements*

Date	Flight track	Starting point	Below-cloud aerosol start time (hhmm, UTC)	Below-cloud aerosol end time (hhmm, UTC)	PCASP (cm^{-3})	k	C (cm^{-3})	CN (cm^{-3})	C/CCN	ε eq. (2)	ε (PDH)
19 June	W/E	southern tip of Tenerife	1534	1546	na	0.8 (±0.2)	270 (±40)	555	0.5	na	
24 June	N/S	north coast of Tenerife (PDH)	1504	1514	na	0·7 (±0.3)	140 (±40)	482	0.3	na	
26 June	60 km square	north of Tenerife	1211	1409	na	1.0 (±0.1)	130 (±10)	218	0.6	na	
4 July	60 km square	north of Tenerife	1400	1552	na	1.1 (±0.1)	200 (±20)	699	0·3	na	
7 July	SW/NW	northern tip of Tenerife	1402	1530	na	0.9 (±0·1)	1300 (±200)	3314	0.4	na	
9 July	60 km square	north of Tenerife	1333	1500	na	0.4 (±0.2)	520 (±120)	636	0.8	na	
17 July	60 km square	north of Tenerife	1210	1312	212	0.9 (±0.1)	550 (±40)	564	1.0	0.3	0.6
18 July	60 km square	north of Tenerife	1337	1536	341	1.1 (±0.1)	750 (±80)	982	0.8	0.2	0.7
19 July	60 km square	north of Tenerife	944	1030	166	0.6 (±0.1)	340 (±30)	516	0.7	0.5	0.9

Tabulated values include the below-cloud averaging interval, integral number concentration measured by the PCASP ($D > 0.1$ μm), the fitted parameters C and k and their statistical uncertainty, the CN concentration and the ratio of the parameter C to the CN concentration. The fit of C and k was restricted to values of S less than 1%. Values of the water soluble mass fraction (ε) inferred from PCASP and CCN measurements, via (2), and derived from measurements of submicrometric composition conducted at the Punto del Hidalgo (PDH) monitoring site (Putaud et al., 2000) are presented in the last columns. The PDH soluble fraction was evaluated as organic anions, sulfate, nitrate, seasalt and ammonium divided by the sum of organic anions, sulfate, nitrate, seasalt, ammonium, organic carbon, black carbon and dust.

north of Tenerife (26 June, 4 July, 9 July, 17 July, 18 July, and 19 July), a flight conducted along a north-south track extending from the north coast of Tenerife (24 June), a flight conducted along a track extending from the northern tip of Tenerife (7 July), and a flight conducted along a westerly track extending from the southern tip of Tenerife (19 June).

4. Summary of aerosol data

Below-cloud aerosol measurements are summarized in Table 1. The measurements from the PCASP were only available for the flights conducted on 17, 18, and 19 July. The PCASP number concentration values for these 3 days, presented in the 6th column, are in excess of $150\,cm^{-3}$. These values of the accumulation mode aerosol concentration are indicative of a moderately polluted airmass. This conclusion is substantiated by the baseline aerosol measurements and airmass trajectory data presented by Putaud et al. (2000).

The WYOCCN measurements from the below-cloud portions of the flights were fitted to the form $N_{ccn} = CS^k$. The fitted parameters, C and k, are given in the 7th and 8th columns of Table 1. These only represent the activation spectrum at values of S less than 1%. We restrict the fit to this range of supersaturation because the observed droplet concentrations very rarely exceeded CCN measurements made at supersaturations larger than 1%. Furthermore, a more detailed fitting function is needed for parameterizing CCN measurements made over the whole range of applied supersaturation (0.2 to 1.6%) (Cohard et al., 1998). Comparisons of the derived values of C and k to the results of Twomey and Wojciechowski (1968) indicate that a mix of both polluted continental and clean maritime airmasses was sampled during ACE-2. The observed minimum and maximum values of C confirm this. The average value of k (0.8) is larger than both the maritime (0.5) and continental (0.6) median values presented by Twomey and Wojciechowski, but is consistent with the continental measurements reported by Braham (1974). Shown in the 10th column of Table 1 is the ratio of C divided by the CN concentration. Pruppacher and Klett (1997) have summarized maritime observations of this parameter. The range of values (0.3 to 1.0) and the average (0.6) are both consistent with published measurements. Also presented in the 7th and 8th columns of Table 1 are statistical uncertainties in the fitted values of C and k. Error in the prediction of the CCN concentration from the equation $N_{ccn} = CS^k$ is typically smaller than $\pm 30\%$.

To facilitate a discussion of the degree of consistency among the CN, CCN and accumulation mode aerosol measurements we present the result from 17 July (Fig. 1). These data were acquired during the below-cloud sampling interval specified in Table 1. For the comparison of the PCASP and the WYOCCN, we have integrated the differential PCASP spectra (dN/dD) and thus obtained cumulative spectral values for each of PCASP size channels ($N(D)$) and for each of the below-cloud measurements. Furthermore, we have employed a relationship between size and critical supersat-

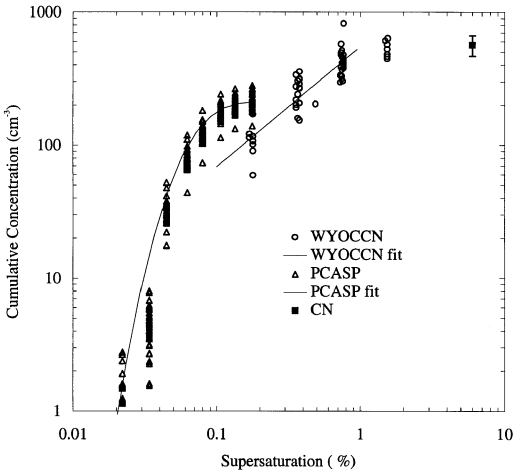

Fig. 1. Below-cloud aerosol concentration measurements derived from the PCASP, the WYOCCN, and the CN counter on 17 July 1997. The CCN data at $S < 1\%$ are fitted to the form $N_{ccn} = CS^k$. The line shows the fitting function; C and k are given in Table 1. PCASP size thresholds were converted to critical supersaturation using (1) on the assumption that the detected particles were composed of ammonium sulfate. Data for only the smallest 8 sizes detected by the PCASP are shown (0.10, 0.12, 0.14, 0.17, 0.20, 0.25, 0.30 and 0.40 μm). The single mode lognormal fitting parameters are median diameter = 0.18 μm, geometric standard deviation = 1.35, and average integral concentration = $212\,cm^{-3}$. CN concentration measurements are plotted at $S = 6\%$, i.e., the value predicted by (1) for ammonium sulfate at the minimum detectable size of 0.01 μm. Error bars on the CN measurements correspond to ± 1 standard deviation.

uration (S_c) which assumes that the particles are composed of ammonium sulfate

$$S_c = 0.00533 D^{-1.51}. \quad (1)$$

Here, S_c is expressed as a percent and the dry particle diameter (D) is in micrometer. Eq. (1) is a parameterization based on Köhler theory (Chylek and Wong, 1998) and laboratory measurements of the composition-dependence of water activity, solution density and surface tension for the $(NH_4)_2SO_4/H_2O$ system (Tang and Munkelwitz, 1994; Pruppacher and Klett, 1997). Our assumption that the CCN active component is ammonium sulfate is consistent with the ACE-2 measurements (Putaud et al., 2000), but it should be recognized that other substances are present and may influence the number concentration of the CCN both by enhancing droplet nucleation or by inhibiting it. The result obtained by transforming the PCASP differential size spectrum to a cumulative activation spectrum is shown in Fig. 1 (triangles). These data were also averaged and fitted to a lognormal size distribution function. The fitting function is illustrated and the fitted parameters are presented in the figure caption.

The concentration comparison at $S \approx 0.2\%$ (PCASP to WYOCCN) indicates that only a subset of the aerosol measured by the PCASP functions as CCN (assuming an external mixture of soluble and insoluble particles). Another possibility is that the aerosol detected by the PCASP exists as an internal mixture of water insoluble and soluble materials. Given the 2- to 3-day transport times from continental source regions (Johnson et al., 2000), we feel that the internal mixture model is most appropriate for the aerosol sampled between 17 and 19 July. Assuming the aerosol is internally mixed, we have inferred the water soluble mass fraction (ε) which reconciles the measurement disparity seen between $S = 0.2\%$ and $S = 0.4\%$ in Fig. 1. This calculation is a 3-step process. First, we calculated the supersaturation value (S^*) corresponding to the integral PCASP measurement if shifted horizontally to intersect the $N_{ccn} = CS^k$ curve. Second, S^* was used to calculate the diameter D^* from (1). Third, the value of ε was calculated as

$$\varepsilon = \rho_{AS} D^{*3} / (\rho_{AS} D^{*3} + \rho_X (D^3 - D^{*3})). \quad (2)$$

Here, D is the minimum size detectable by the PCASP (0.10 μm) and ρ_{AS} and ρ_X are the bulk densities of ammonium sulfate (1.78 gm/cm^3) and the insoluble component (assumed to be 1.3 gm/cm^3 (Putaud et al, 2000)), respectively. Our 2nd step requires the assumption that the insoluble component makes an insignificant contribution to the size of the embryo at the critical supersaturation. This assumption is corroborated by calculations presented in Table 6.3 of Pruppacher and Klett (1997). The calculated soluble fractions are presented in the penultimate column of Table 1. We note that these values are reduced by more than a factor of 2 if the minimum detectable PCASP size recommended by Liu et al. (1992) (0.14 μm) is employed in the calculation. Values of ε based on measurements of the composition of the submicrometric aerosol are presented in the final column of Table 1. The fact that the derived values of ε are substantially smaller than values inferred from the chemical analysis suggests that a component of the aerosol may inhibit droplet activation. This speculation and the apparent inverse correlation between the derived values of ε and number concentration are consistent with long-term studies of aerosol properties at Cape Grim, Tasmania (Bigg, 1986; Gras, 1995). In spite of the disparity between the derived aerosol solubility and the chemical composition measurement, we note that the WYOCCN data are constrained by the PCASP concentration measurements in a manner that is qualitatively consistent with the size detection threshold of the PCASP and Köhler theory. The same can be said of the comparison between the CN and the $S = 1.6\%$ WYOCCN data, provided particles larger than 0.01 μm but smaller than 0.03 μm make a small contribution to the CN concentration. This is generally true for marine boundary layer conditions over the Atlantic Ocean (Hoppel et al., 1990).

5. Case study — 17 July 1997

A specific example of the Merlin aerosol and cloud microphysical measurements is shown in Figs. 2a–f. In the 1st panel (Fig. 2a) we plot the pressure altitude of the aircraft and provide symbols which indicate the position of the aircraft along the 60 km square. The data shown in Figs. 2a–f were collected during a turn at the northern corner of the 60 km square (labeled ***N***), during a level traverse of the cloud layer from ***N*** to the

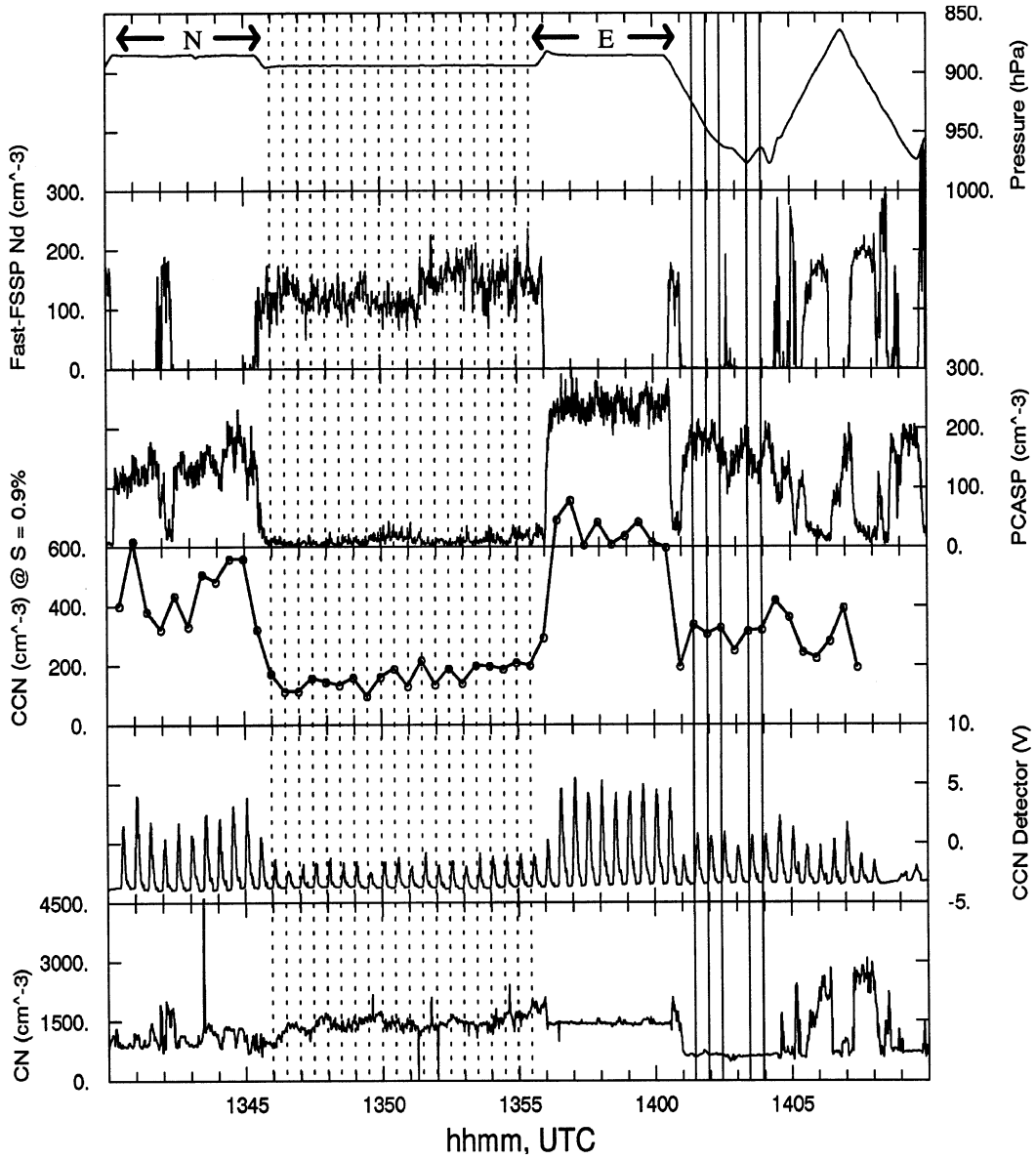

Figs. 2(a) (top panel) to (f) (bottom panel). Aerosol and cloud microphysics measurements from a section of the 60 km square flown on 17 July 1997. The upper panel shows the pressure altitude of the Merlin and the location of the Merlin along the square (***N*** = northern corner and ***E*** = eastern corner). The panels (b) through (f) illustrate the fast-FSSP measurement of droplet concentration, the PCASP measurement of accumulation mode aerosol concentration, the WYOCCN measurement of CCN concentration ($S = 0.9\%$), the CCN photodetector voltage, and the CN concentration, respectively. Dashed vertical lines indicate CCN (and PCASP) sample times during the cloud traverse and solid vertical lines indicate CCN (and PCASP) samples from below-cloud. We screened the CCN and PCASP sample intervals which were conducted below the average cloud base (910 hPa) and eliminated those that were influenced by the presence of the cloud droplets (for example at 14:03 UTC).

eastern tip of the square (labeled ***E***), during a turn at ***E***, and during an ascent/descent maneuver conducted from ***E*** to the southern tip of the square. We note that the Merlin arrived at the southern way point at 14:11 UTC. In the remaining panels we plot the fast-FSSP measurement of droplet concentration (Fig. 2b), the PCASP number concentration (Fig. 2c), the CCN concentration at $S = 0.9\%$ (Fig. 2d), the CCN photodetector voltage (Fig. 2e), and the CN concentration (Fig. 2f). Dashed vertical lines delineate CCN flush intervals which occurred during the cloud traverse and solid vertical lines delineate flush intervals corresponding to below-cloud sampling. The CCN measurements derived from both the cloud-interstitial and below-cloud sampling intervals are examples of the type of data used in the following section to estimate droplet concentration by difference. We emphasize that this technique of inferring N_d is based on level-flight traverses of the cloud and that the below-cloud data was obtained from the closest available measurements. The time interval between the cloud-interstitial and the below-cloud measurements was restricted to 20 min.

As is discussed in the previous paragraph, the Merlin made turns in the free-troposphere above the cloud layer. Data collected during these time intervals are indicated by the **N** and **E** in Fig. 2a. Compared to the measurements made in the free-troposphere, smaller CCN concentrations were observed in the below-cloud layer. Positive vertical gradients in the CCN were also evident during the mission flown in background marine conditions on 26 June. For the flight conducted on 17 July, free-tropospheric aerosol and CCN concentrations were most enhanced in the vicinity of the eastern corner of the 60-km square. This result points to the existence of a more polluted airmass aloft, particularly along the eastern extent of the measurement domain on 17 July. However, no enhancement of below-cloud aerosol or CCN were evident at this same location when observations were made at $\sim$13:00 UTC. The fact that the boundary layer appears to be isolated from free-tropospheric influences, at least on the 2- to 4-h time scale of a research flight, is not surprising considering the large thermal stability at cloud top. Clearly, the simplest approach is to assume that there is minimal interaction between the aerosol that exits within the free troposphere and within the boundary-layer. If this assumption is valid then differences between the below-cloud and cloud-interstitial CCN measurements should be comparable to the direct measurements of droplet concentration. This is the basis for the comparison presented in the following section.

One additional aspect of the Merlin data set is evident in Fig. 2f. As was previously discussed, the CN was sampled from a reverse-flow inlet. The CN measurement shows cloud-interstitial concentrations increasing by a factor of 2 to 5 relative to the below-cloud values. Following the work of Hudson and Frisbie (1991) and Clarke et al. (1997), we attribute the in-cloud CN enhancement to cloud droplet shattering either on the upwind surface of the inlet or subsequent to droplet aspiration. No evidence was found by either Hudson and Frisbie or Clarke et al., or in our analysis of the ACE-2 data set from the Merlin, indicating that accumulation mode concentration or CCN concentration at low to moderate supersaturation are enhanced by this phenomenon.

6. Below-cloud and interstitial aerosols: comparisons to the fast-FSSP

As was previously mentioned, the Merlin conducted several long traverses (30 to 60 km) of the cloud layer. These were followed by a descent, similar to that shown in Fig. 2a, or by a series of rapid ascent/descent maneuvers separated by short-duration (30 to 90 s) sampling intervals either below or above the cloud layer. Furthermore, we have seen that a decrease in either the CCN or accumulation mode aerosol concentration is evident when comparing below-cloud and cloud-interstitial measurement intervals. This decrease is presumably due to the fact that particles which participate in the condensation process grow to sizes which are too large to be sampled by either of the inlets. Therefore, one check for consistency in the data set is to compare the direct measurement of N_d with values derived by differencing the below-cloud and cloud-interstitial CCN measurements. With the exception of the flights conducted on 4 July, 7 July and 9 July, this comparison was possible for all the flights summarized in Table 1.

The comparison technique is summarized in Fig. 3. First we note that droplet activation con-

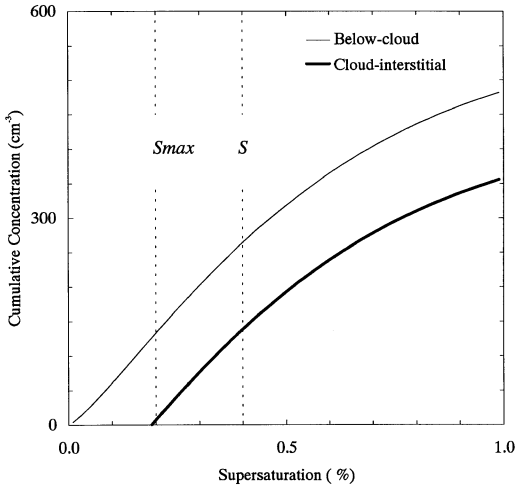

Fig. 3. The effect of droplet activation on the CCN spectrum. Note that the difference between below-cloud and cloud-interstitial concentrations yields the cloud droplet concentration if the maximum environmental supersaturation (S_{max}) is less than the applied supersaturation (S).

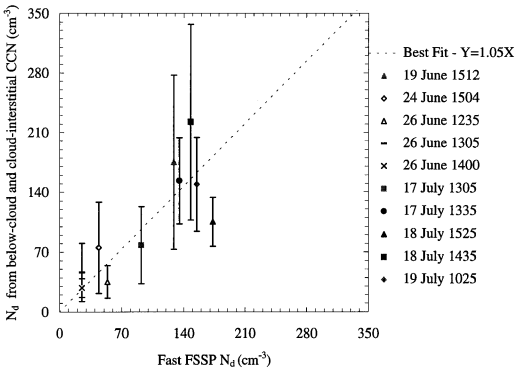

Fig. 4. Compared values of N_d derived from both WYOCCN and fast-FSSP measurements. The inferred values of N_d (y-axis) were obtained by differencing the concentrations of below-cloud and cloud-interstitial CCN. Error bars correspond to the root-mean-square error resulting from variability in both the below-cloud and cloud-interstitial measurements. The standard error in the slope of the best-fit line is ± 0.11.

verts a fraction of the CCN population to cloud droplets. In natural clouds the distinction between CCN that initiate droplet growth and those that remain as interstitial particles occurs at the maximum environmental supersaturation (S_{max}). This property is controlled by both the vertical velocity and the CCN activation spectrum. According to this conceptual model the droplet concentration can be estimated by differencing below-cloud and cloud-interstitial CCN measurements. A necessary condition is that the applied supersaturation (S) must exceed. S_{max}. We evaluated S_{max} using the maximum observed value of N_d, plus C and k, and we found that only half of the available data segments were consistent with the $S_{max} < S$ constraint. However, when we evaluated S_{max} using the average N_d plus one standard deviation, plus C and k, all of the available data points met the $S_{max} < S$ constraint. The result is illustrated in Fig. 4. We note that the 2 points which plot farthest from the best-fit line (26 June 1235 and 18 July 1525) came closest to the limiting constraint. Their position below the best-fit line is therefore consistent with the conceptual model shown in Fig. 3.

Fig. 4 demonstrates that there is good agreement between the predicted and observed values of N_d. This implies that the CCN and the fast-FSSP concentration measurements are consistent, that there are no substantial biases associated with the cloud-interstitial CCN sampling technique, and that the droplet activation process feeds on a local supply of sub-cloud aerosol. Further confirmation of the latter inference comes from the results obtained from 2 flights (26 June and 17 July) which were characterized by larger above-cloud CCN concentrations compared to that observed within the below-cloud layer. Data points corresponding to these 2 flights are not systematically biased relative to the one-to-one line. The observed consistency for these 2 cases reinforces our hypothesis of weak coupling between the free-tropospheric and marine boundary layer aerosol fields.

7. Measured and calculated droplet concentration

Studies of cumulus clouds conducted by Twomey and Warner (1967), and by Fitzgerald and Spires-Duran (1973) show good agreement between measured droplet concentrations and predictions based on measurements of updraft velocity and below-cloud CCN. The theory that links the CCN, w and N_d has been reviewed by Johnson (1981). Clearly both vertical velocity and the CCN

are important determinants of N_d. Although this dependence is expected to hold for stratocumulus cloud systems, the statistical characteristics of the updraft differs from that observed within cumulus. For example, maximum updraft velocities are smaller and the relative variability of the velocity is larger within stratocumulus. These characteristics of vertical velocity field in stratocumulus suggest that N_d closure studies should be expressed in terms of the 1st, 2nd, and possibly the 3rd moment of the N_d probability density function (pdf). This view of the activation process recognizes that a dispersion of N_d values is produced for one aerosol type, and is consistent with observations from the ACE-2 Cloudy-Column campaign (Brenguier et al., 1999). These authors have also demonstrated that N_d is affected by entrainment but not to a degree that exceeds the variability in N_d which originates from the droplet activation process. Following this approach we now examine measurements of w, N_d and droplet spectra from the 13 level-flight cloud traverses summarized in Table 2.

First we were interested in seeing if there was a relationship between w and N_d consistent with the predictions of condensation theory. The correlation coefficients shown in the 6th row of Table 2 indicate that w and N_d are positively correlated. This correlation is weakest for the cleanest case (26 June) and strongest for the most polluted case (7 July) and for the cumulus cloud studied on 4 July. These findings are consistent with the work of Gilliani et al. (1995) which show that the fraction of aerosols activated to droplets is a weak function of vertical velocity, under clean conditions, and a much stronger function of w when aerosol concentrations are typical of polluted conditions. The existence of a positive correlation between w and N_d suggests that the cloud retains a memory of the droplet activation process. This conjecture was explored further by stratifying the time series into samples that correspond to the upper and lower 10% of the vertical velocity values. Comparisons were then made between 3 properties of the droplet size spectrum: number concentration, droplet size dispersion (i.e., standard deviation divided by the average), and cloud liquid water content (LWC) derived from integration of the fast-FSSP spectra. The final 3 rows of Table 2 demonstrate that (1) N_d is larger for those samples associated with the upper 10% of vertical velocity values, (2) that the dispersion is smaller for these samples, and (3) that the LWC is usually larger. A specific example of this phenomenon is presented in Fig. 5. Observe that the spectrum sampled from the regions associated with the largest values of w is narrow and is also shifted to smaller size in comparison to the spectrum sampled from regions associated with the strongest downdrafts. We speculate that this difference results from the fact that parcels moving rapidly upwards have recently passed through cloud base. The observed narrow droplet spectra support this inference. Furthermore, parcels associated with the smallest values of w have presumably had longer residence time within the cloud and are therefore more likely to have intermixed with cloud parcels of different thermodynamic and kinematic origin or with dry air at cloud top. These inferences are consistent with the analysis conducted by Hudson and Svensson (1995), and with the expected consequences of dry air entrainment, i.e., the production of downdrafts and the reduction of N_d.

The proceeding discussion demonstrates that vertical velocity can be used to select cloud sections which have characteristics that are anticipated for condensational growth in isolation from

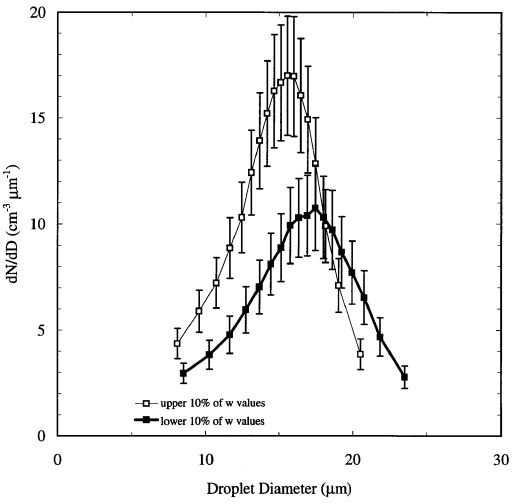

Fig. 5. Droplet size spectra sampled from the cloud traverse conducted 13:46 to 13:56 UTC on 17 July 1997. The sampling is based on the measured vertical velocity. Error bars correspond to ± 1 standard deviation. This variability results from pooling spectra from different regions of the cloud.

Table 2. *Cloud traverse intervals*

Date	19 June	24 June	26 June	26 June	26 June	4 July	7 July	7 July	9 July	17 July	17 July	18 July	19 July
cloud traverse start time (hhmmss UTC)	151254	151518	124638	142015	132009	142057	144500	151416	135300	131300	134600	154500	103200
clould traverse end time (hhmmss UTC)	151613	152106	125630	142349	132220	142157	145800	151852	140400	132359	135539	155209	104359
median vertical velocity (m/s)	−0.03	0.40	0.22	0.51	0.28	2.22	0.11	0.22	0.25	0.01	0.16	0.05	0.11
vertical velocity standard deviation (m/s)	0.94	0.26	0.34	0.27	0.24	1.36	0.28	0.59	0.46	0.30	0.29	0.48	0.41
N_d/w correlation coefficient	0.34	0.14	0.09	0.20	0.19	0.77	0.62	0.43	0.22	0.44	0.42	0.36	0.45
updraft N_d larger than downdraft N_d?	yes	yes	yes	yes	yes	yes	yes	yes	yes	yes	yes	yes	yes
updraft droplet spectrum broader than downdraft droplet spectrum?	yes	yes	yes	yes	yes	yes	yes	yes	yes	yes	yes	yes	yes
updraft LWC larger than downdraft?	yes	no	yes	no	yes	yes	yes	yes	yes	no	no	yes	yes

other perturbing processes. We now consider values of N_d extracted from cloud regions characterized by values of w greater than the median value (Table 2, 4th row) and compare this distribution to calculations based on the Twomey equation. The sets of w used in the calculation also correspond to values greater than the median, however these were adjusted by subtracting the median. The velocity adjustment isolates the turbulent component of the vertical motion field from mesoscale forcing and measurement bias. (We note, however, that no velocity adjustment was made for the data collected in the cumulus cloud studied on 4 July; for this case the large median value (2.2 m/s) is physically significant.) In addition to the set of adjusted updraft values, the CCN parameters C and k (Table 1) were used as inputs to the Twomey equation. We have utilized the following form of the Twomey equation (Pruppacher and Klett, 1997)

$$N_d = C^{2/(k+2)} \left[\frac{0.069 w^{3/2}}{kB(k/2, 3/2)} \right]^{k/(k+2)} . \quad (3)$$

In (3), B is the beta function, C and N_d are in cm^{-3}, and w is in cm/s.

The comparison of the calculated and measured values of N_d is shown in Fig. 6. Also illustrated is the best-fit line described by $Y = 0.9X$. The statistical uncertainty in the slope of the best-fit line is ± 0.09. On average we are therefore able to infer

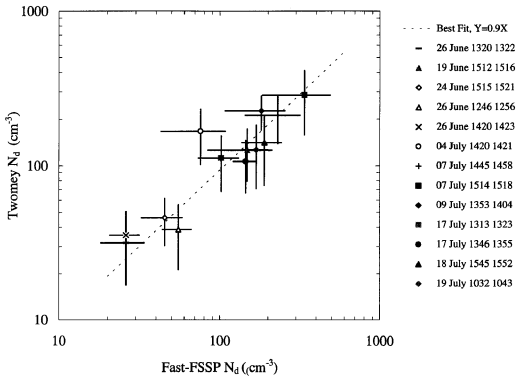

Fig. 6. Compared values of N_d calculated using the Twomey equation and that measured using the fast-FSSP. For this comparison, only fast-FSSP measurements associated with vertical velocities larger than the median value were used to infer the plotted average and standard deviation. The standard error in the slope of the best-fit line is ± 0.09.

N_d within the uncertainty of the CCN ($\pm 40\%$) and the vertical velocity measurements (± 0.1 m/s). The point associated with the largest departure from the overall trend comes from data collected within the cumulus cloud studied on 4 July. This departure is discussed in the following section. In Fig. 6, we represent the observed and predicted N_d standard deviations with error bars.

For about half of the plotted data points our approach correctly reproduces the N_d standard deviation observed by the fast-FSSP. This aspect of the intercomparison implies that the width of the vertical velocity pdf is consistent with the width of the droplet concentration pdf. The implication is that the observed variability in the selected values of N_d is strongly influenced by variability in vertical velocity at cloud base. Data points characterized by larger predicted N_d standard deviations, compared to that observed, may result from uncertainties in the shape of the CCN spectrum or from the fact that only the largest observed updraft values are representative of that which produce activation at cloud base. Distinguishing between these 2 possibilities will be necessary for improving model parameterizations of the droplet activation process.

8. Discussion

Measurements of both below-cloud CCN and accumulation mode aerosol are presented in Table 1. Using Köhler theory, we have derived values of the soluble mass fraction which force agreement between those 2 data sets. This comparison yields values of ε which are significantly smaller than values based on measurements of the submicrometric aerosol composition. This result is shown in the final 2 columns of Table 1. Bigg (1984) and Gras (1995) observed similar disparities and show that it is most pronounced when airmass trajectories bring polluted air to a coastal maritime sampling location in Tasmania. One possible implication of this result is that calculations of the activation supersaturation based on Köhler theory and measurements of aerosol size and composition are inconsistent with supersaturation values that actually produce activation within the WYOCCN. This would imply that condensation is slowed by films (Bigg, 1986), that the form of the relationship used to predict the

Köhler curve is incorrect (Chylek and Wong, 1998), or that there are non-ideal chemical effects due to the internal mixing of aerosol components (Winkler, 1973). Errors in the calibration of CCN counters could also explain the disparity, but these would presumably produce overprediction of the number density as often as underprediction, whereas the latter appears to be the case for most of the aerosol/CCN closure attempts that have been published. Clearly each of these issues needs to be investigated so that the link between aerosols and CCN can be strengthened. Having said this, it is also important to realize that both vertical velocity and the CCN activation spectrum control N_d. It is therefore important to incorporate both effects into predictions of cloud albedo and to also evaluate the sensitivity of the result to the uncertainties in the transformation between the aerosol size and CCN activation supersaturation.

We have also presented a set of measured droplet concentration values and show that these are consistent with calculations based on CCN and vertical velocity. The degree of consistency is comparable to that found in studies of both cumulus (Twomey and Warner, 1967; Fitzgerald and Spires-Duran, 1973) and stratocumulus (Yum et al., 1998). We emphasize that the current study has focused on a relationship that couples the CCN activation spectra, w and N_d. Validated relationships between aerosol physicochemical properties and droplets will require further analysis of the ACE-2 data set. This work will need to be tempered with the recognition that there is generally poor agreement between measurements of CCN and aerosol both in previous studies (Bigg, 1986; Quinn et al., 1993; Covert et al., 1998) and in the analyses of data collected during ACE-2 (Chuang et al., 2000; Wood et al., 2000).

The observed scatter seen in Fig. 6 may be due to the ± 0.1 m/s error in the measurement of vertical velocity, to systematic bias in our assessment of below-cloud CCN, or to errors resulting from the assumptions implicit in the Twomey equation. Somewhat surprisingly the cloud associated with the largest vertical velocity values (4 July) exhibited the largest discrepancy between predicted and observed values of N_d. This would seem to implicate one or both of the last 2 sources of uncertainty as the reason for the observed discrepancy. Johnson (1981) has characterized the errors in N_d that result from the simplifying assumptions made in deriving the Twomey equation. These result from the use of only 2 parameters to describe the activation spectrum and from the fact that droplet growth is postponed until the supersaturation passes an appropriate critical value. Continued modeling work, similar to that conducted by both Johnson (1981) and by Feingold and Heymsfeld (1992), is needed to examine the possibility that some of the scatter seen in Fig. 6 can be attributed to inaccuracies resulting from the activation spectrum parameterization or other limitations of the Twomey approach.

9. Summary and conclusions

Below-cloud measurements of CCN made with a new airborne counter, the WYOCCN, during 9 flights conducted as part of the ACE-2 Cloudy-Column initiative have been analyzed. Data was collected both in unpolluted and moderately polluted airmasses. Data from the latter environment were compared to concurrent measurements of the accumulation mode aerosol. Based on this comparison we have documented a factor of 2 or larger difference between the concentrations of CCN at $S = 0.2\%$ and the concentration of aerosol larger than 0.1 μm. Values of the aerosol soluble fraction (ε) that range between 0.2 and 0.5 are needed to explain the concentration difference. Since the derived values of ε are substantially smaller than direct composition measurements, it is concluded that a disparity exits between the concentration of particles that function as CCN within a static diffusion cloud chamber and those that are predicted to function as CCN based on measurements of the aerosol size spectrum and composition. A further analysis of the extensive set of aerosol physicochemical property measurements from ACE-2 together with vertical velocity and droplet concentration is needed to better understand the sensitivity of predicted droplet concentration values to this disparity.

Local values of the below-cloud CCN measurements were compared to cloud interstitial measurements, and by difference, were used to infer the cloud droplet concentration. Comparisons of the inferred values of N_d with measurements obtained from the fast-FSSP exhibit a level of agreement which is consistent with the observed spatial vari-

ability of the below-cloud CCN. Although the sampling of dry particle sizes smaller than ~ 0.02 μm is complicated by an apparent particle production artifact resulting from droplet shattering (Hudson and Frisbie, 1991), future use of the cloud-interstitial sampling technique may provide insight into the apparent aerosol/CCN disparity.

The principal focus of this paper has been the comparison of directly measured values of droplet concentration with values computed using the Twomey equation. Uncertainties in the values of vertical velocity used in the Twomey equation were minimized by using data sampled from level-flight traverses of the cloud layer. Values of w acquired in this manner were found to be positively correlated with N_d and the correlation coefficient was larger for airmasses containing higher concentrations of CCN. We based the comparison of measured and computed droplet concentration on w values sampled from cloud regions containing vertical velocity values larger than the cloud traverse median. Using the C/k parameterization of the activation spectrum we obtained reasonably good agreement between the observation and the calculation. This result indicates that there is consistency among the measurements of CCN, vertical speed and droplet concentration. Emphasis now needs to be placed on aerosol physical and chemical property measurements and their relationship to N_d via activation parameterizations. The hope is that this work will lead to improvements in the simulation of marine stratocumulus albedo.

10. Acknowledgements

We would like to thank J. P. Putaud for providing the aerosol composition data. Thanks are also extended to Andreas Petzold and Franz Schröder for their collaboration during the field experiment, for the data that they shared openly, and their advice. Funding support from the National Science Foundation (grant ATM-98 16119), the European Community and Meteo France are also recognized.

REFERENCES

Albrecht, B. 1989. Aerosols, cloud microphysics, and fractional cloudiness. *Science* **245**, 1227–1230.

Bigg, E. K. 1986. Discrepancy between observation and prediction of concentrations of cloud condensation nuclei. *Atmos. Res.* **20**, 82–86.

Boers, R. and Mitchell, R. M. 1994. Adsorption feedback in stratocumulus clouds: influence on cloud top albedo. *Tellus* **46A**, 229–241.

Braham, R. R. Jr. 1974. Cloud physics of urban weather modification — a preliminary report. *Bull. Amer. Meteor. Soc.* **55**, 100–106.

Brenguier, J. L., Bourrianne, T., Coelho, A. A., Isbert, J., Peytavi, R., Trevarin, D. and Wechsler, P. 1998. Improvements of the droplet size distribution measurements with the Fast-FSSP. *J. Atmos. Oceanic Technol.* **15**, 1077–1090.

Brenguier, J. L., Pawlowska, H., Schüller, L., Preusker, R., Fischer, J. and Fouquart, Y. 1999. Radiative properties of boundary layer clouds: droplet effective radius versus number concentration. *J. Atmos. Sci.*, in press.

Brown, E. N., Friehe, C. A. and Lenschow, D. H. 1983. The use of pressure fluctuations on the nose of an aircraft for measuring air motion. *J. Clim. Appl. Meteorol.* **22**, 171–180.

Chuang, P. Y., Collins, D. R., Pawlowska, H., Snider, J., Jonsson, H. H., Brenguier, J. L., Flagan, R. C. and Seinfeld, J. H. 2000. CCN measurements during ACE-2 and their relationship to cloud microphysical properties. *Tellus* **52B**, 843–867.

Chylek, P. and Wong, J. G. D. 1998. Erroneous use of the modified Köhler equation in cloud and aerosol physics applications. *J. Atmos. Sci.* **55**, 1473–1477.

Clarke, A. D., Uehara, T. and Porter, J. N. 1997. Atmospheric nuclei and related aerosol fields over the Atlantic: clean subsiding air and continenetal pollution during ASTEX. *J. Geophys. Res.* **102**, 25,281–25,292.

Cohard, J.-M., Pinty, J.-P. and Bedos, C. 1998. Extending Twomey's analytical estimate of nucleated cloud droplet concentrations from CCN spectra. *J. Atmos. Sci.* **55**, 3348–3357.

Covert, D. S., Gras, J. L., Wiedensohler, A. and Stratmann, F. 1998. Comparisons of directly measured CCN and CCN modeled from the number-size distribution in the marine boundary layer during ACE-1 at Cape Grim, Tasmania. *J. Geophys. Res.* **103**, 16,597–16,608.

Dobosy, R. J., Crawford, T. L., MacPherson, J. I., Desjardins, R. L., Kelly, R. D., Oncley, S. P. and Lenschow, D. H. 1997. Intercomparison among four flux aircraft at BOREAS in 1994. *J. Geophys. Res.* **102**, 29,101–29,111.

Feingold, G. and Heymsfeld, A. 1992. Parameterizations of the condensational growth of droplets for use in GCMs. *J. Atmos. Sci.* **49**, 2325–2342.

Fitzgerald, J. W. and Spyers-Duran, P. 1973. Changes

in cloud nucleus concentration and cloud droplet size distribution associated with pollution from St. Louis. *J. Appl. Meteor.* **30**, 511–516.

Fitzgerald, J. W., Hoppel, W. A., Gelbard, F. 1998. A one-dimensional sectional model to simulate multicomponent aerosol dynamics in the marine boundary layer (1). Model description. *J. Geophys. Res.* **103**, 16,085–16,102.

Foltescu, V. L., Selin, E. and Below, M. 1995. Corrections for particle losses and sizing errors during aircraft aerosol sampling using a Rosemount inlet and the PMS LAS-X. *Atmos. Environ.* **29**, 449–453.

Ghan, S. J., Chuang, C. C. and Penner, J. E. 1993. A parameterization of cloud droplet nucleation part I: single aerosol type. *Atmos. Res.* **30**, 198–221.

Gilliani, N. V., Schwartz, S. E., Leaitch, W. R., Strapp, J. W. and Isaac, G. A. 1995. Field observations in continental stratiform clouds: partitioning of cloud particles between droplets and unactivated interstitial aerosols. *J. Geophys. Res.* **100**, 18,687–18,706.

Gras, J. L. 1995. CN, CCN and particle size in southern ocean air at Cape Grim. *Atmos. Res.* **35**, 233–251.

Gultepe, I., Isaac, G. A., Leaitch, W. R. and Banic, C. M. 1996. Parameterizations of marine stratus microphysics based on in situ observations: implications for GCMs. *J. Climate* **9**, 345–357.

Hoppel, W. A., Fitzgerald, J. W., Frick, G. M. and Larson, R. E. 1990. Aerosol size distributions and optical properties found in the marine boundary layer over the Atlantic Ocean. *J. Geophys. Res.* **95**, 3659–3686.

Hudson, J. G. and Svensson, G. 1995. Cloud microphysical relationships in California marine stratus. *J. Atmos. Sci.* **34**, 2655–2666.

Hudson, J. G. and Frisbie, P. R. 1991. Cloud condensation nuclei near marine stratus. *J. Geophys. Res.* **96**, 20,795–20,808.

Huebert, B. J., Lee, G. and Warren, W. L. 1990. Airborne aerosol inlet passing efficiency measurement. *J. Geophys. Res.* **95**, 16,369–16,381.

Johnson, D. B. 1981. Analytical solutions for cloud-drop concentration. *J. Atmos. Sci.* **38**, 215–218.

Johnson et al. 2000. An overview of the Lagrangian experiments undertaken during the north Atlantic regional Aerosol Characterization Experiment (ACE-2). *Tellus* **52B**, 290–320.

Lala, G. G. and Jiusto, J. E. 1977. An automatic light scattering CCN counter. *J. Appl. Meteor.* **16**, 413–418.

Liu, P. S., Leaitch, W. R., Strapp, J. W. and Wasey, M. A. 1992. Response of particle measuring systems airborne ASASP and PCASP to NaCl and latex particles. *Aerosol Sci. Technol.* **16**, 83–95.

Paluch, I. R. and Lenschow, D. H. 1991. Stratiform cloud formation in the marine boundary layer. *J. Atmos. Sci.* **48**, 2141–2158.

Pruppacher, H. R. and Klett, J. D. 1997. *Microphysics of clouds and precipitation.* Kluwer, Dordrecht.

Putaud, J. P., Van Dingenen, R., Mangoni, M., Virkkula, A. and Raes, F. 2000. Chemical mass closure and origin assessment of the submicron aerosol in the marine boundary layer and the free troposphere at Tenerife during ACE-2. *Tellus* **52B**, 141–168.

Quinn, P. K., Covert, D. S., Bates, T. S., Kapustin, V. N., Ramsey-Bell, D. C. and McInnes, L. M. 1993. Dimethylsulfide/cloud condensation nuclei/climate system: relevant size-resolved measurements of the chemical and physical properties of atmospheric aerosol particles. *J. Geophys. Res.* **98**, 10,411–10,427.

Raes, F. 1995. Entrainment of free tropospheric aerosols as a regulating mechanism for cloud condensation nuclei in the remote marine boundary layer. *J. Geophys. Res.* **100**, 2893–2903.

Raes, F., Bates, T., McGovern, F. and Van Liedekerke, M. 2000. The 2nd Aerosol Characterization Experiment (ACE-2). General context and main results. *Tellus* **52B**, 111–126.

Schröder, F. and Ström, J. 1997. Aircraft measurements of submicrometer aerosol particles (>7 nm) in the midlatitude free troposphere and tropopause region. *Atmos. Res.* **44**, 333–356.

Snider, J. R. et al. 2000. Comparisons of four cloud condensation nucleus measurement systems. *J. Atmos. Oceanic Technol.*, submitted.

Tang, I. N. and Munkelwitz, H. R. 1994. Water activities, densities, and refractive indices of aqueous sulfates and sodium nitrate droplets of atmospheric importance. *J. Geophys. Res.* **99**, 18,801–18,808.

Twomey, S. 1959. The nuclei of natural cloud formation. Part II: the supersaturation in natural clouds and the variation of cloud droplet concentration. *Geophy. Pura. Appl.* **43**, 243–249.

Twomey, S. 1977. *Atmospheric aerosols.* Elsevier, New York.

Twomey, S. and Warner, J. 1967. Comparison of measurements of cloud droplets and cloud nuclei. *J. Atmos. Sci.* **24**, 702–703.

Twomey, S. and Wojciechowski, T. A. 1968. Observations of the geographical variation of cloud nuclei. *J. Atmos. Sci.* **26**, 684–688.

Winkler, P. 1973. The growth of atmospheric aerosol particles as a function of the relative humidity (II). An improved concept of mixed nuclei. *Aerosol Sci.* **4**, 373–387.

Wood, R. et al. 2000. Boundary layer and aerosol evolution during the 3rd Lagrangian experiment of ACE-2. *Tellus* **52B**, 401–422.

Yum, S. S., Hudson, J. G. and Xie, Y. 1998. Comparisons of cloud microphysics with cloud condensation nuclei spectra over the summertime southern ocean. *J. Geophys. Res.* **103**, 16,625–16,636.